# NASA TECHNICAL MEMORANDUM

NASA TM X-71578

NASA TM X-71578



# SUPPRESSOR NOZZLE AND AIRFRAME NOISE MEASUREMENTS DURING FLYOVER OF A MODIFIED F106B AIRCRAFT WITH UNDERWING NACELLES

by Richard R. Burley
Lewis Research Center
Cleveland, Ohio 44135

TECHNICAL PAPER proposed for presentation at
Winter Annual Meeting of the American Society
of Mechanical Engineers
New York, New York, November 17-22, 1974

# SUPPRESSOR NOZZLE AND AIRFRAME NOISE MEASUREMENTS DURING FLYOVER OF A MODIFIED F106B AIRCRAFT WITH UNDERWING NACELLES

by Richard R. Burley*

## ABSTRACT

The effect of flight velocity on the jet noise and thrust of a 104-tube suppressor nozzle was investigated using an F-106B delta wing aircraft modified to carry two underwing nacelles each containing a turbojet engine. The nozzle was mounted behind one of the nacelles. Flight velocity had a large adverse effect on thrust and a small adverse effect on suppression when correlated with relative jet velocity. The clean airframe noise of the aircraft was measured at Mach 0.4 and was compared with that predicted from an empirical expression. The 83 dB measured value was considerably below the predicted value.

E-8028

## INTRODUCTION

Two important aspects of the noise problem associated with advanced supersonic transport aircraft are the effect of flight velocity on jet noise and the amount of noise generated by the airframe itself. Concerning jet noise, it has been the practice to evaluate exhaust nozzles used to suppress jet noise on the basis of static tests (cf. Refs. [1] to [3]).** However, when the maximum sideline noise is reached during takeoff, the flight speed of these aircraft can be as high as Mach 0.35. At these flight speeds, external air flowing across the nozzle could effect its

*Lewis Research Center, National Aeronautics and Space Administration, 21000 Brookpark Road, Cleveland, Ohio 44135.

**Numbers in brackets designate References at end of paper.

noise and thrust. Concerning airframe noise, it has recently been suggested[4] that the noise generated by the airframe as it moves through the air might constitute a noise floor beyond which quieting the engines would be ineffective. Some studies of airframe noise have been done using aircraft designed for subsonic speeds.[4-8] Aircraft designed for supersonic speeds, however, might have a considerably different level of airframe noise since their wing planform is significantly different.

To investigate the effect of flight velocity on jet noise and thrust, flyover and static tests using a modified F-106B aircraft are being conducted on a wide variety of both unsuppressed and suppressed type exhaust nozzles. Some of the results are reported in References [9] to [15]. Tests of a 104-tube suppressor nozzle have recently been completed. In connection with these tests, the airframe noise of the F-106B aircraft was determined and was compared with that predicted from an existing empirical relationship. The purpose of this paper is to present and discuss the results in both of these areas.

The F-106B aircraft is a delta wing aircraft designed for a maximum speed of Mach 2 in level flight. The aircraft has been modified to carry two underwing nacelles each containing a calibrated J85-GE-13 turbojet engine. The 104-tube suppressor nozzle was mounted behind one of these nacelles and its gross thrust minus drag determined from a load cell measurement. The flyovers were conducted at an altitude of 300 feet (91 m) and a Mach number of 0.4. The landing gear was retracted. Acoustic measurements were taken from a ground station beneath the flight path. For static tests, the acoustic measurements were taken at a radial distance of 100 feet (30.5 m) from the nozzle. The main engine of the aircraft, a J75

turbojet engine, was at idle power for both the flyover and the static tests.

## APPARATUS AND PROCEDURE

### F-106B Aircraft

Flyover and static tests were conducted using an F-106B delta wing aircraft modified to carry two underwing nacelles. Figure 1 shows the aircraft in flight and Table I gives dimensional data. The aircraft was about 71 feet (22 m) long with a wing span of about 38 feet (12 m) and weighed about 38 000 pounds (17 000 kg). The wing had an approximately 4 percent thick NACA 000-65 airfoil section, a mean aerodynamic chord of about 24 feet (7 m), and an aspect ratio of 2.2. The leading edge of the wing was sweptback $60^{\circ}$.

Figure 2 shows a schematic view of the nacelle-engine installation. The 25-inch (63.5-cm) diameter nacelles were mounted to the wing aft lower surface by two attachment links on each side of the fuselage at approximately 32 percent semispan with the exhaust nozzles extending beyond the wing trailing edge. Each nacelle,which contained a calibrated J85-GE-13 turbojet engine, had normal shock inlets with blunted cowl lips for the flyover tests. Secondary air to cool the engine was supplied from the inlet and was controlled at the periphery of the compressor face by a calibrated rotary valve. For the static tests, the blunted cowl lips were replaced with a bellmouth and the secondary air was supplied from an external source. A load cell technique[16] was used to measure nacelle thrust minus drag to determine exhaust nozzle performance for both flyover and static tests.

Engine airflow was determined by using the calibration results from

Reference [17] along with measurements of engine speed and total pressure and temperature at the compressor face. Fuel flows were obtained from calibrated flowmeters. Conditions at the primary nozzle exit ($P_8$,$T_8$,$A_8$) were computed knowing airflow, turbine discharge conditions, and fuel flow rates.

An onboard digital data system (described in Ref. [16]) recorded pressures, temperatures, and load cell output on magnetic tape. A flight calibrated test boom located on the aircraft nose was used to determine free-stream static and total pressure, aircraft angle of attack, and yaw angle. Aircraft speed was obtained from a calibrated Machmeter.

## Noise Measurements

Microphones for both the flyover and the static tests were 1-inch (2.54-cm) diameter ceramic type. Their frequency response was flat to within ±2 dB for grazing incidence over the frequency range used (50 to 10 000 hertz). The output of the microphones was recorded on a two-channel direct record tape recorder. The entire system was calibrated for sound level in the field before and after each test using a conventional tone calibrator. The tape recorder was calibrated for linearity with a "pink" noise (constant energy per octave) generator.

Both the flyover and static signals were recorded on magnetic tape. The tape was played back through one-third-octave-band filters and then reduced to digital form. The averaging time for data reduction was 0.1 second for the flyover signal and 0.125 second for the static signal.

Meteorological conditions, in terms of dry-bulb and dewpoint temperatures, wind speed and direction, and barometric pressure were recorded periodically throughout the tests. Wind speeds were less than 10 knots

(5.144 m/sec) during all tests.

Noise measurements for the flyover tests were made from a ground station beneath the flight path (Fig. 3(a)). The microphone, which was fitted with a windscreen that caused no loss of signal, was positioned 4 feet (1.22 m) above a concrete surface. It was oriented to receive the acoustic pressure wave at grazing incidence.

The geometry of the flyover is shown in Figure 3(b). As the aircraft travels along its flight path, the direct ray distance from the suppressor nozzle to the microphone, $R_p$, continuously changes as does the angle between the direct ray and the jet exit centerline, referred to as the acoustic angle $\theta$. The values of $R_p$ and $\theta$ shown in Figure 3(b) assume the aircraft flies directly over the microphone at an altitude of exactly 300 feet (91 m). (Ref. [11] discusses the reasons for selecting this altitude.) Since this may not always be the case, provisions were made to adjust the recorded sound pressure level to these conditions. The technique required a camera located adjacent to the microphone. The camera recorded a picture of the aircraft as it passed overhead; at the same time a 14 kilohertz signal was recorded on the tape. (Further details of the technique are given in Ref. [18].)

The flyovers were conducted at a Mach number of 0.4. The main engine of the aircraft (J75) was at idle power while the data were being recorded. For the suppressive nozzle tests, the J85 engine in the nacelle that contained this nozzle was operated over a range of power settings; the J85 engine in the other nacelle was shut off and windmilling. The background noise level of the aircraft during flyover was established with both J85 engines shut off and windmilling.

The location of the microphone for the static tests is shown in Figure 4. The microphone was positioned 4 feet (1.22 m) above the concrete surface and was oriented to receive the acoustic pressure wave at normal incidence (Fig. 4(a)). It was fitted with a windscreen that caused no loss of signal. The acoustic measurements were taken at a radial distance of 100 feet (30.5 m) from the exhaust nozzle exit in increments of $10^{o}$ over a $90^{o}$ sector (Fig. 4(b)). During the measurements, the main engine was at idle power. For the suppressor nozzle tests, the J85 engine in the nacelle that contained this nozzle was operated over a range of power settings; the J85 engine in the other nacelle was shut off. The background noise level at static conditions was determined with both J85 engines shut off.

## Suppressor Nozzle

The suppressor nozzle, which was a 104-tube configuration designed for use with an auxiliary inlet ejector nozzle (Fig. 5), was tested with an acoustically treated shroud and with no shroud. The suppressor configuration was patterned after a Boeing Company design described in Reference [19].

The suppressor configuration without a shroud is shown in Figure 5(a). The tubes have an elliptical shape and are mounted on a conical baseplate with the tube major axis in the radial direction. The area ratio, that is, the ratio of the area circumscribing the suppressor nozzle to the primary nozzle effective area, is 2.8. The tubes are divided into five rows with all tubes in a given row having the same length. The tubes in the outer row are the longest, and the ventilation factor, that is, the ratio of the side flow area between the outer row of tubes to the base area, is

about 0.6. Conceptually, the array of tubes would be divided into four hinged segments. For unsuppressed operation these segments would swing out of the primary jet and be stowed in the space around the primary nozzle.

The suppressor configuration with the acoustic shroud is shown in Figure 5(b). The acoustic treatment consisted of a perforated plate adjacent to the hot jet, a bulk absorber made of stainless steel wire mesh, and a solid backing plate. The acoustic shroud had a maximum cavity depth of 1.81 inches (4.57 cm). The outer surface of the shroud had a boattail angle of $10^{o}$. (Further details of this nozzle are given in Ref. [18].)

## RESULTS AND DISCUSSION

### Suppressor Nozzle

The effect of flight velocity on the noise of a 104-tube suppressor nozzle was studied by comparing the flyover and static spectra after they were adjusted to the same conditions of 100 feet (30.5 m) from the nozzle in the free-field on a standard day. The Doppler shift of frequency was accounted for in the flyover spectra and caused a maximum shift of frequency of one 1/3-octave-band. (Details of the adjustments are given in Ref. [11].) The comparison was made at a constant relative jet velocity of 1760 feet per second (536 m/sec) and at a constant jet velocity of 2200 feet per second (670 m/sec) for the acoustic angle that resulted in peak flyover noise. A relative jet velocity of 1760 feet per second (536 m/sec) corresponds to a jet velocity of 2200 feet per second (670 m/sec) for the flyover condition. This, in turn, corresponds to about military power setting of the J85 engine.

In comparing the spectra, the greatest emphasis is placed on the data

at frequencies between 160 and 5000 hertz. At frequencies below 160 hertz, the sample size is small due to the short integration time, the narrowness of the frequency bands, and the rapidly changing conditions of the flyover. Consequently, the results are less reliable. At frequencies above 5000 hertz, the acoustic signal received at the ground station quite possibly is below the noise floor of the recording equipment. Values of the atmospheric absorption coefficient are very large at these high frequencies and multiply the noise floor to unrealistically high noise levels when the flyover data are adjusted to the distance of 100 feet (30.5 m) from the nozzle.

Comparison of flyover and static spectra were made at the same relative jet velocity and at the same jet velocity. This was done to indicate, for this suppressor nozzle, whether low frequency noise might correlate with relative jet velocity and high frequency noise with jet velocity. It was based on Reference [5] which suggested a correlating parameter for use with ejector-suppressor nozzles; the noise aft of the ejector shroud (i.e., low frequency noise) might be expected to correlate with relative jet velocity and the noise generated within the ejector shroud (i.e., high frequency noise) might be expected to correlate with elemental jet velocity minus secondary air velocity.

Comparison of the flyover and static spectra at the same relative jet velocity is shown in Figure 6. Figure 6(a) shows the results for the suppressor configuration without a shroud. The flyover spectrum was very close to the static spectrum from frequencies of 160 to 630 hertz suggesting that relative jet velocity might be a proper correlating parameter for the low frequency noise. The high frequency peak value for the

flyover (which occurred at 4 kilohertz) was only about 1.5 dB higher than that for the static spectrum suggesting that the high frequency portion might also correlate with relative jet velocity. In the midfrequency range (800 to 2500 hertz) however, the flyover spectrum was considerably above the static spectrum principally because a dip occurred in the static spectrum at a frequency of about 1250 hertz. This dip was in the region where the first cancellation would be expected to occur and the method for adjusting to free-field probably undercorrects for this (Ref. [11] gives the method for correcting to free-field). Another possible reason is that the spectrum has both a low frequency peak and a high frequency peak which is characteristic of suppressor nozzles. The intersection of these two segments of the spectrum seemed to occur at a frequency of about 1250 hertz. Because of these differences, the OASPL and PNL values were about 2 dB higher for the flyover than for the static spectrum suggesting that flight velocity had a small adverse effect on suppression of the configuration without a shroud. Figure 6(b) shows the results for the configuration with the acoustic shroud. The low frequency portion of the spectrum (160 to 630 hertz) again seemed to correlate with relative jet velocity. The high frequency portion, however, did not correlate with relative jet velocity since the flyover spectrum was significantly higher than the static spectrum. The flyover spectrum also was considerably higher than the static spectrum in the midfrequency range. This again was due mainly to the dip in the static spectrum at 1250 hertz. These differences resulted in an OASPL value of 2 dB higher and a PNL value of 3 PNdB higher for the flyover than for the static spectrum. It suggests that flight velocity also had an adverse effect on suppression of the configuration

with an acoustic shroud. The adverse effect seems to be slightly greater with the acoustic shroud than without it. Furthermore, the low frequency portion of the spectra seemed to correlate reasonably well with relative jet velocity regardless of whether the acoustic shroud was installed. The high frequency portion of the spectrum for the configuration without a shroud also appeared to correlate with relative jet velocity.

Comparison of the flyover and static spectra at the same jet velocity is shown in Figure 7. Figure 7(a) presents the results for the configuration without a shroud. The flyover spectrum is substantially below the static spectrum over the frequency range of principle interest except in the vicinity of 1250 hertz where it is somewhat above the static spectrum. This difference resulted in OASPL and PNL values that were about 3 dB lower for the flyover than for the static spectrum. It suggests that flight velocity had a small beneficial effect on suppression of the configuration without the acoustic shroud. Figure 7(b) shows the results for the configuration with the acoustic shroud. The flyover spectrum was substantially below the static spectrum from frequencies of 160 to 630 hertz and markedly above it in the vicinity of 1250 hertz. At higher frequencies, the two spectra were very close suggesting that jet velocity might be a proper correlating parameter for the high frequency noise. As a result of the differences at the low and mid frequencies, the OASPL value was 2 dB lower and the PNL value was 1 PNdB lower for the flyover than for the static spectrum. It suggests that flight velocity had a very small beneficial effect on suppression of the configuration with the acoustic shroud. The beneficial effect seemed to be somewhat greater without the acoustic shroud than with it. Also, the high frequency por-

tion of the spectra for the configuration with the acoustic shroud seemed to correlate reasonably well with jet velocity.

Another indication of flight velocity effect was obtained by comparing the flyover and static results in terms of the variation in perceived noise level with acoustic angle. Figure 8 presents the results for a typical flyover at an altitude of 300 feet (91 m) compared to that predicted from static data extrapolated from the 100 feet (30.5 m) radius at which the data were taken to the 300 feet (91 m) sideline. The results are shown for the same relative jet velocity and for the same jet velocity. Figure 8(a) shows the results for the configuration without a shroud. The flyover noise level reached a peak value of about 111 PNdB at an acoustic angle of about $70^{\circ}$. Static results at the same relative jet velocity predicted a somewhat lower peak value (109.5 PNdB) occurring about $10^{\circ}$ closer to the jet axis. Static results at the same jet velocity, however, predicted a higher peak value (114.5 PNdB) occurring at about the same acoustic angle as that for the flyover results. Figure 8(b) shows the results for the configuration with the acoustic shroud. The flyover noise level reached a peak value of about 108 PNdB at an angle of about $70^{\circ}$. Static results at the same relative jet velocity predicted a lower peak value (104 PNdB) occurring slightly (about $5^{\circ}$) further away from the jet axis. Static results at the same jet velocity, however, predicted a slightly higher peak value (109 PNdB) occurring at about the same acoustic angle as that for the flyover.

In addition to the effect of flight velocity on noise, it is also important to know how flight velocity affects thrust. The thrust coefficient of the suppressor at flyover and static conditions is shown in

Figure 9 as a function of exhaust nozzle pressure ratio and the corresponding jet velocity. Flight velocity had a large adverse effect on the thrust coefficient over the entire range of pressure ratios. At a pressure ratio of 2.46 ($V_j$ = 2200 fps (670 m/sec)), the thrust coefficient of the configuration without a shroud decreased from 0.90 at static conditions to 0.835 for flyover conditions; the adverse effect became even more pronounced as pressure ratio decreased. The adverse effect of flight velocity was due largely to the increased pressure drag on the baseplate. The configuration with the acoustic shroud also experienced an adverse effect. At a pressure ratio of 2.46, the thrust coefficient decreased from 0.92 at static conditions to 0.835 at flyover conditions; the adverse effect again became somewhat more pronounced as pressure ratio decreased. The principal reason for the adverse effect for the configuration with the acoustic shroud was the ram drag associated with bringing the external air into the ejector at flyover conditions.

Although flight velocity adversely affected the thrust coefficient of both configurations, the configuration with the acoustic shroud experienced the greater adverse effect. Installing the acoustic shroud increased the thrust coefficient at static conditions to 0.92 from 0.90 because the shroud acted as an ejector but had no effect on the thrust coefficient at flyover conditions which remained at 0.835.

The acoustic data from the flyover tests were scaled up from J85 engine size (0.23 scale) to full size (four 60 000 lb, 267 kN thrust engines) using the Strouhal number relationship and then adjusted to a sideline distance of 2128 feet (648 m) from an altitude of 1000 feet (305 m). Jet noise suppression was obtained by referencing these noise levels to

those from a plug nozzle scaled in a like manner (Ref. [11] describes plug nozzle). The effect on suppression of scaling and of increasing the distance between the noise source and the observer is shown in Figure 10 for the suppressor configuration with the acoustic shroud. Scaling up to full size increased suppression by about 2 PNdB. The higher more annoying frequencies were more dominant for the suppressor nozzle than for the reference plug nozzle. Scaling up to a larger nozzle shifted these frequencies into a lower less annoying range resulting in the increased suppression. The effect of increasing the distance between the noise source and the observer was to increase suppression by an additional 3 PNdB. The high frequencies contribute more to the perceived noise level of the suppressor nozzle than they did to the reference nozzle, and it is these high frequencies that are attenuated by the atmosphere. Also shown in this figure is the effect of time duration on suppression. Noise from this suppressor nozzle had a somewhat shorter time duration which reduced the annoyance by 1 EPNdB compared to the reference plug nozzle.

Suppressor effectiveness in terms of effective perceived noise level as a function of percent thrust loss is presented in Figure 11 for the flyover data scaled up to full size. The suppressor was more effective with the acoustic shroud than without it. With the acoustic shroud, a suppression of 14.5 EPNdB was achieved for a thrust loss of 14.3 percent. Removing the acoustic shroud reduced suppression to 12.5 EPNdB but did not change the thrust loss.

This probably is not the peak noise suppression achievable with this suppressor. The design on which this suppressor was based had its peak noise suppression for static conditions at a jet velocity of about

2500 feet per second (762 m/sec) and a pressure ratio of 3.[19] This jet velocity and pressure ratio cannot be achieved at nonafterburning conditions for the J85 engine.

## Airframe Noise

The discussion so far has been concerned with the effect of flight velocity on the jet noise and thrust of a suppressor nozzle. As part of these tests, which were done using a modified F-106B delta wing aircraft, the background noise level of this aircraft was measured during flyover.

The results are shown in figure 12 in terms of the variation in perceived noise level with acoustic angle. For comparison, the flyover noise levels of the suppressor configurations are also shown (repeated from fig. 8). In the region of peak noise level for the suppressor nozzle ($\theta = 70^{o}$), the background noise level of the aircraft is sufficiently low so it does not interfere with noise from the suppressor nozzles. The background noise level reached a peak value of 98 PNdB at an angle of $110^{o}$. The peak noise level is fairly flat, changing only about 1 PNdB between acoustic angles of $130^{o}$ and $90^{o}$. The noise generated at an acoustic angle of $110^{o}$ arrived at the microphone at the same time that the aircraft passed over the microphone. This agrees with a result of Reference 4 where the peak noise level was heard when the aircraft was overhead.

The frequency spectra associated with this background noise level are shown in figure 13 for acoustic angles in the region of peak noise. Also shown is the frequency spectrum associated with the background noise level at static conditions. The source of this noise is the J75 engine operating at idle power. The static spectrum has been adjusted from the

100 foot radius at which the measurements were taken to the 300 foot (91 m) sideline to be consistent with the 300 foot (91 m) altitude of the flyover.

The segment of the flyover spectra between frequencies of 200 and 1250 hertz is considered to be due to airframe noise. It is broadband with a peak value of 73 dB occurring at a frequency of about 570 hertz.

Airframe noise is defined as what remains after accounting for all other noise sources. One of these nonairframe noise sources is discrete tones due to the rotational speed of the engines. These tones, which occur at frequencies corresponding to blade passing frequencies of the turbine as well as the first few stages of the compressor, were responsible for the noise in the mid-to-high frequency part of the flyover spectra.

The other nonairframe noise source is broadband noise associated with the highly turbulent flow of the exhaust gases inside the tailpipe (internally generated noise) and the turbulent mixing of the exhaust jet with the surrounding air (jet mixing noise). This noise from the J75 engine, which operates at idle power, was identified from the static tests. The spectrum is shown in figure 13. Broadband noise reached a peak value of 65 dB at a frequency of about 125 hertz. The spikes at frequencies above 1 kilohertz were due to discrete tones from the rotating machinery. Noise from the J75 engines at idle power does not significantly influence airframe noise since its level is at least 10 dB below airframe noise over most of the frequency range of interest.

Broadband noise also emerges from the exhaust nozzle of the windmilling J85 engines, and it is also low enough so as not to influence airframe noise. Because the exhaust gases are not heated, the internally

generated noise and the jet mixing noise are lower than that from the J75 engine, which is itself insignificant in the frequency range of interest.

Now that the airframe noise has been identified, an important question concerns how it compares with predictions. An empirical method for predicting airframe noise was given in Reference 4. The empirical method was based on tests of five aircraft designed for low subsonic speeds. The aircraft were a Prue-2 sailplane, Cessna 150, Aero-Commander Shrike, Douglas DC-3, and a Convair 240; gross weight ranged from 1300 to 38 000 pounds (590 to 17 700 kg) and airspeed varied from 98 to 325 feet per second (30 to 99 m/sec). The resulting empirical relationship for overall sound pressure level of an aerodynamically "clean" configuration was:

$$\text{OASPL} = 10 \log_{10}\left[K \times \frac{V_a^4}{h^2} \times \frac{w}{c_L} \times \frac{C}{b}\right] + 8.4, \text{ dB}$$

Since gross weight, w, is essentially equal to lift which is proportional to the second power of aircraft velocity, the OASPL is proportional to the sixth power of aircraft velocity. The measured spectrum was broadband and peaked at a frequency given by:

$$f = 1.095 \frac{V_a}{t_m}, \text{ hertz}$$

Since airfoil thickness, $t_m$, was found to correlate as the relevant length factor in the Strouhal number and because of the dipole nature of the noise, it was concluded in Reference 4 that the predominant noise source was wing trailing-edge vortex shedding. (Ref. 20 suggests that, at these high Reynolds numbers, the noise is caused by random surface-pressure fluctuations associated with the turbulent boundary layer on the wing rather than from the shedding vortices.) These empirical relations were

applied to a very large subsonic aircraft with a sweptback wing in Reference 6 (a C-5 Galaxy), and were successful in predicting the "clean" airframe noise and the frequency where the broadband spectrum peaked.

How successful these relations are in predicting the airframe noise of an F-106B delta wing aircraft designed for supersonic speeds is shown in Figure 14. The segment of the measured airframe spectrum from Figure 7 has been extrapolated down to 50 hertz and up to 10 kilohertz and OASPL and PNL values calculated. The empirical relationship successfully predicted the frequency where the broadband spectrum peaked. However, the empirical expression was not successful in predicting the "clean" airframe noise level. The predicted value was about 20 dB too high.

Although the reasons for this are not yet known, significant differences exist between the present test and those of Reference 4 in terms of the values of the aircraft parameters. The three aircraft parameters of interest are aircraft speed, $V_a$, the ratio of mean chord to span, C/b, and wing area, S (the wing area parameter is obtained by substituting the expression $c_L = 2w/S\rho V_a^2$ into the equation for OASPL). The range over which these aircraft parameters were investigated in Reference 4 in developing the empirical relation for OASPL is shown on the abscissa of Figure 15 along with the corresponding values for the F-106B test. The ordinate of the figure gives the predicted noise contribution of the aircraft parameter. Of the three parameters only the wing area of the F-106B was within the range investigated in Reference 4. Flight speed of the F-106B aircraft was somewhat higher than the speed of the aircraft in Reference 4. The greatest difference, however, was in the value of mean chord to span ratio, which is the reciprocal of the aspect ratio. The

F-106B aircraft has a low aspect ratio, 2.2, due to its delta wing, whereas the aircraft of Reference 4 have straight or tapered wings with relatively high aspect ratios of between about 7 and 18.

Also shown in Figure 15 are the values of the aircraft parameters for the C-5 Galaxy tested in Reference 6. Of the three parameters only wing area was outside the range investigated in Reference 4. Although the wing area was very much greater than those of Reference 4, the empirical relations successfully predicted the "clean" airframe noise and the frequency where the spectrum peaked. This was not the case for the F-106B delta wing aircraft. It suggests that the "clean" airframe noise might be more sensitive to changes in aspect ratio (such as occur in going from a tapered to a delta wing) than to large changes in the area of the wing.

Recent flyover noise measurements of a Lockheed Jet Star (ref. 21) indicated that its "clean" airframe noise level was about the same as that of the F-106B aircraft. The Jet Star, which has about the same gross weight and wing area as the F-106B aircraft, has a sweptback wing platform with an aspect ratio of 5.27. This suggests that the delta wing platform of the F-106B aircraft probably is not primarily responsible for its low airframe noise although the low aspect ratio still might be a large factor.

## CONCLUSIONS

A modified F-106B aircraft was used to investigate the effect of flight velocity on the jet noise and thrust of a 104-tube suppressor

nozzle. In connection with these tests, the "clean" airframe noise of the aircraft was determined and was compared with that predicted from an existing empirical relationship. The following results were obtained.

Suppressor Nozzle

1. Flight velocity can have either an adverse or a beneficial effect on noise suppression of this suppressor configuration depending on whether the comparison was made at the same relative jet velocity or at the same jet velocity. Comparing the flyover and static spectra at the same relative jet velocity resulted in an adverse effect (about 3 PNdB for the suppressor with the acoustic shroud). A slight beneficial effect resulted when compared at the same jet velocity (about 1 PNdB for the suppressor with the acoustic shroud).

2. Flight velocity had a large adverse effect on thrust coefficient. The thrust coefficient decreased from 0.92 at static conditions to 0.835 at a Mach number of 0.4 for the suppressor with the acoustic shroud (nozzle pressure ratio of 2.46).

3. Noise suppression effectiveness, in terms of perceived noise level at a sideline distance of 2128 feet (648 m) for engines scaled to full size, achieved a value of 14.5 EPNdB for a thrust loss of 14.3 percent.

Airframe Noise

1. The maximum noise level of the "clean" airframe was 83 dB. The associated spectrum was broadband and peaked at a frequency of about 570 hertz.

2. An existing empirical expression successfully predicted the frequency where the spectrum peaked. However, the empirical expression was not successful in predicting the maximum airframe noise level. The pre-

dicted value was about 20 dB too high.

## SYMBOLS

| | |
|---|---|
| $A_8$ | primary nozzle exit effective flow area, $in.^2$ ($cm^2$) |
| AR | aspect ratio, b/C |
| b | wing span, ft (m) |
| C | mean aerodynamic wing chord, ft (m) |
| $c_L$ | coefficient of lift |
| D | nozzle drag, lb (kN) |
| EPNL | effective perceived noise level, EPNdB |
| F | nozzle thrust, lb (kN) |
| $F_{ip}$ | ideal thrust of primary jet, lb (kN) |
| f | frequency, hertz |
| h | aircraft altitude, ft (m) |
| K | constant equal to 0.123 for English units (2.92 for metric units) |
| $M_0$ | flight Mach number |
| OASPL | overall sound pressure level, dB (re 0.0002 μ BARS) |
| $P_8$ | total pressure at primary nozzle exit, psia ($kN/m^2$) |
| $P_8/P_0$ | nozzle pressure ratio |
| PNL | perceived noise level, PNdB |
| $P_0$ | ambient static pressure, psia ($kN/m^2$) |
| $R_p$ | direct ray distance between exhaust nozzle and microphone, ft (m) |
| S | wing area, $ft^2$ ($m^2$) |
| $T_s$ | total temperature of secondary air, $^oR$ (K) |
| $T_8$ | total temperature at primary nozzle exit, $^oR$ (K) |
| $t_m$ | mean wing thickness, ft (m) |
| $V_a$ | aircraft velocity, ft/sec (m/sec) |

$V_j$ ideal jet velocity, ft/sec (m/sec)

$V_R$ relative jet velocity, $V_j - V_a$, ft/sec (m/sec)

$W_s$ secondary weight flow, lb/sec (kg/sec)

$W_8$ weight flow at primary nozzle exit, lb/sec (kg/sec)

w aircraft gross weight, lb (kg)

$\alpha$ aircraft angle of attack, deg

$\theta$ angle between direct ray and jet exit centerline, deg

$\rho$ density of air, $lb/ft^3$ ($kg/m^3$)

$\omega\sqrt{\tau}$ corrected secondary weight flow ratio, $\frac{W_s}{W_8}\sqrt{\frac{T_s}{T_8}}$

## REFERENCES


1. Darchuk, G. V., and Balombin, J. R., "Noise Evaluation of Four Exhaust Nozzles for Afterburning Turbojet Engines," NASA TM X 2014, May 1970.

2. Huff, R. G., and Groesbeck, D. E., "Splitting Supersonic Nozzle Flow into Separate Jets by Overexpansion into a Multilobed Divergent Nozzle," NASA TN D 6667, Mar. 1972.

3. Ciepluch, C. C., North, W. J., Coles, W. D., and Antl, R. J., "Acoustic, Thrust and Drag Characteristics of Several Full-Scale Noise Suppressors for Turbojet Engines," NACA TN 4261, 1958.

4. Gibson, J. S., "The Ultimate Noise Barrier - Far Field Radiated Aerodynamic Noise," Proceedings Inter-Noise '72; International Conf. on Noise Control Engineering, Oct. 1972, pp. 332-337.

5. Blumenthal, V. L., Streckenbach, J. M., and Tate, R. B., "Aircraft Environmental Problems," presented at the 1972 AIAA Annual Meeting and Technical Display, 9th, Washington, AIAA Paper No. 73-5.

6. Gibson, J. S., "Non-Engine Aerodynamic Noise Investigation of a Large Aircraft," NASA CR 2378, Oct. 1973.

7. Healy, G. J., "Measurement and Analysis of Aircraft Far-Field Aerodynamic Noise," NASA CR-2377, 1974.

8. Revell, J. D., "The Calculation of Aerodynamic Noise Generated by Large Aircraft at Landing Approach," presented 87th Meeting Acoustical Society of America, 1974, Paper No. JJ9.

9. Burley, R. R., and Karabinus, R. J., "Flyover and Static Tests to Investigate External Flow Effects on Jet Noise for Non-Suppressor and Suppressor Exhaust Nozzles," NASA TM X 68161, Dec. 1972.

10. Brausch, J. F., "Flight Velocity Influence on Jet Noise of Conical Ejector, Annular Plug and Segmented Suppressor Nozzles," General Electric Co., 1972 (also NASA CR-120961).

11. Burley, R. R., Karabinus, R. J., and Freedman, R. J., "Flight Investigation of Acoustic and Thrust Characteristics of Several Exhaust Nozzled Installed on Underwing Nacelles on an F106 Airplane," NASA TM X 2854, Aug. 1973.

12. Chamberlin, R., "Flyover and Static Tests to Study Flight Velocity Effects on Jet Noise of Suppressed and Unsuppressed Plug Nozzle Configurations," NASA TM X 2856, Aug. 1973.

13. Burley, R. R., and Johns, A. L., "Flight Velocity Effects on Jet Noise of Several Variations of a Twelve-Chute Suppressor Installed on a Plug Nozzle," NASA TM X 2918, Feb. 1974.

14. Burley, R. R., and Head, V. L., "Flight Velocity Effects on Jet Noise of Several Variations of a 48-Tube Suppressor Installed on a Plug Nozzle," NASA TM X 2919, Feb. 1974.

15. Wilcox, F. A., "Comparison of Ground and Flight Test Results Using a Modified F106B Aircraft," NASA TM X 71439, Nov. 1973.

16. Groth, H. W., Samanich, N. E., and Blumenthal, P. Z., "Inflight Thrust Measuring System for Underwing Nacelles Installed on a Modified F-106 Aircraft," NASA TM X 2356, Aug. 1971.

17. Antl, R. J., and Burley, R. R., "Steady-State Airflow and Afterburning Performance Characteristics of Four J85-GE-13 Turbojet Engines," NASA TM X 1742, Feb. 1969.

18. Burley, R. R., "Flight Velocity Effects on the Jet Noise of Several Variations of a 104-Tube Suppressor Nozzle," NASA TM X 3049, 1974.

19. Swan, W. C., and Simcox, C. D., "A Status Report on Jet Noise Suppression as Seen by as Aircraft Manufacturer," First International Symposium on Air Breathing Engines, June, 1972.

20. Paterson, R. W., et al "Vortex Shedding Noise of an Isolated Airfoil," Report K910867-6, United Aircraft Corp., Dec. 1971.

21. Lasagna, P. L., and Putnam, T. W., "Preliminary Measurements of Aircraft Aerodynamic Noise," AIAA, Palo Alto, Calif., Paper 74-572, June 1974.

TABLE I. - AIRCRAFT DIMENSIONAL DATA (UNMODIFIED AIRCRAFT)

| | |
|---|---|
| **Wing** | |
| Airfoil section | NACA 0004-65 (Mod.) |
| Span | 38.13 ft (11.62 m) |
| Area (to aircraft ℄) | 697.83 $ft^2$ (64.83 $m^2$) |
| Root chord (at aircraft ℄) | 35.63 ft (10.86 m) |
| Tip chord | 0.94 ft (0.29 m) |
| Mean aerodynamic chord | 23.76 ft (7.24 m) |
| Aspect ratio | 2.2 |
| Taper ratio | 0 |
| Sweepback of L. E. | 60° |
| **Elevons** | |
| Span | 12.85 ft (3.92 m) |
| Area aft of hinge line | 66.6 $ft^2$ (6.2 $m^2$) |
| Root chord | 3.15 ft (0.96 m) |
| Tip chord | 2.03 ft (0.62 m) |
| **Vertical tail** | |
| Airfoil section | NACA 0004-65 (Mod.) |
| Area (total) | 105 $ft^2$ (9.8 $m^2$) |
| Aspect ratio | 0.97 |
| Sweepback of L. E. | 55° |
| **Fuselage** | |
| Length (overall) | 70.75 ft (21.56 m) |
| Height (maximum) | 7.50 ft (2.29 m) |
| Width (maximum) | 8.10 ft (2.47 m) |
| Surface area | 985 $ft^2$ (91.5 $m^2$) |
| **Total airplane surface area** | 2230 $ft^2$ (207.2 $m^2$) |
| **Gross weight (with nacelles)** | 38 000 lb (17 000 kg) |

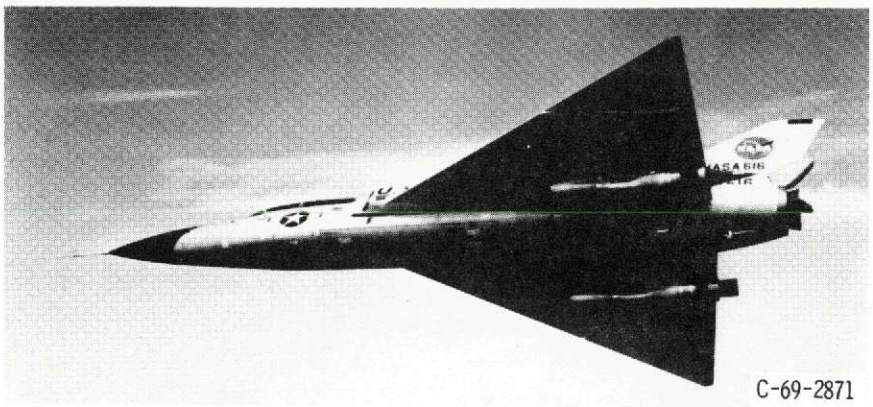


Figure 1. - Modified F-106B aircraft in flight.



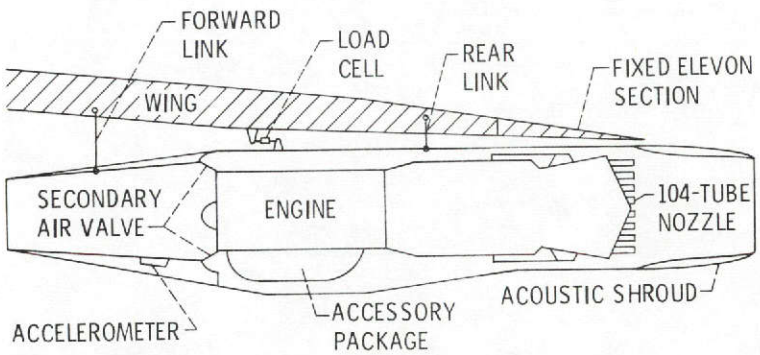


Figure 2. - Nacelle-engine installation.

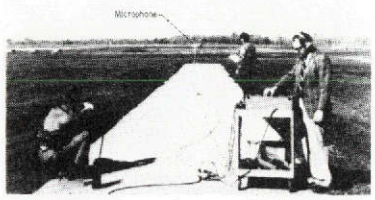


(a) Microphone orientation.

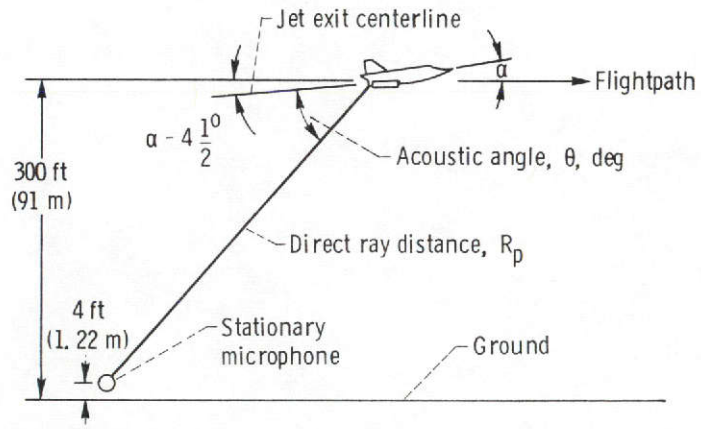


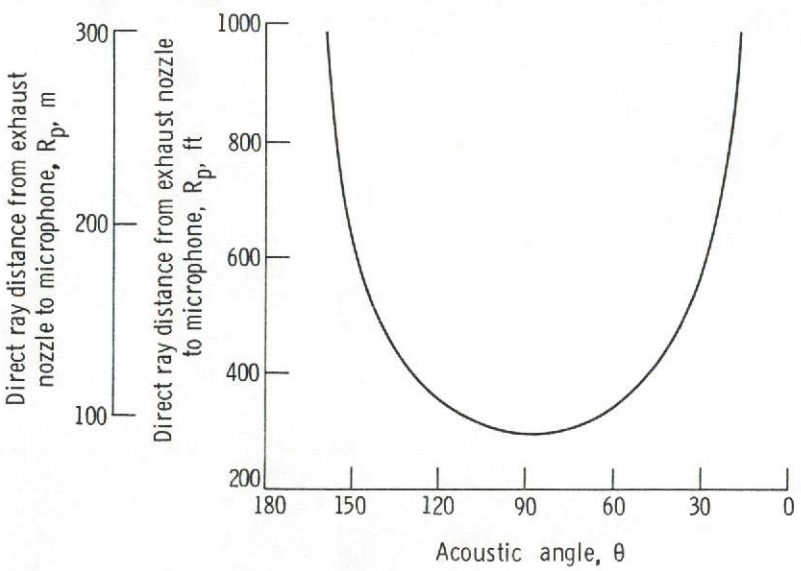


(b) Geometry

Figure 3. - Microphone orientation and geometry for flyover tests.


(a) Microphone orientation.



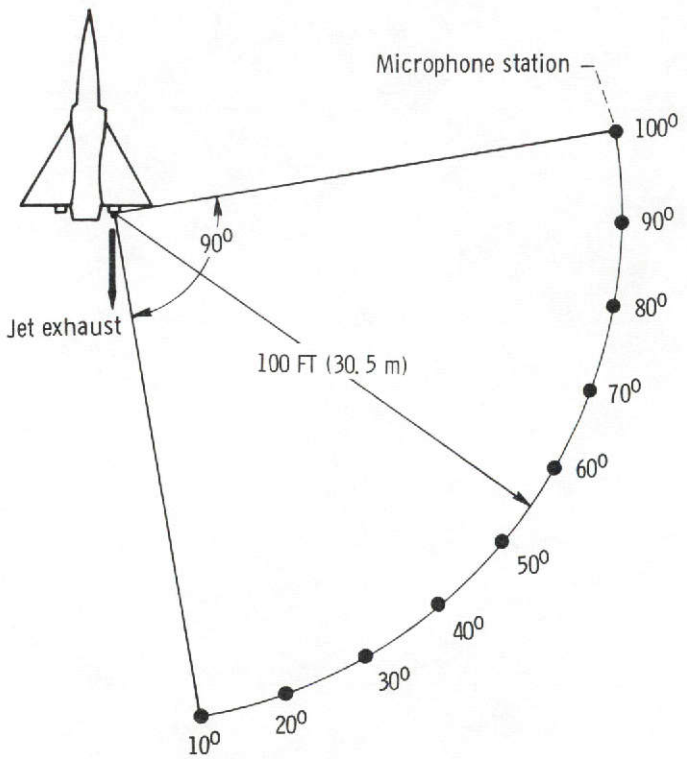


(b) Microphone location.

Figure 4. - Microphone orientation and location for static tests.

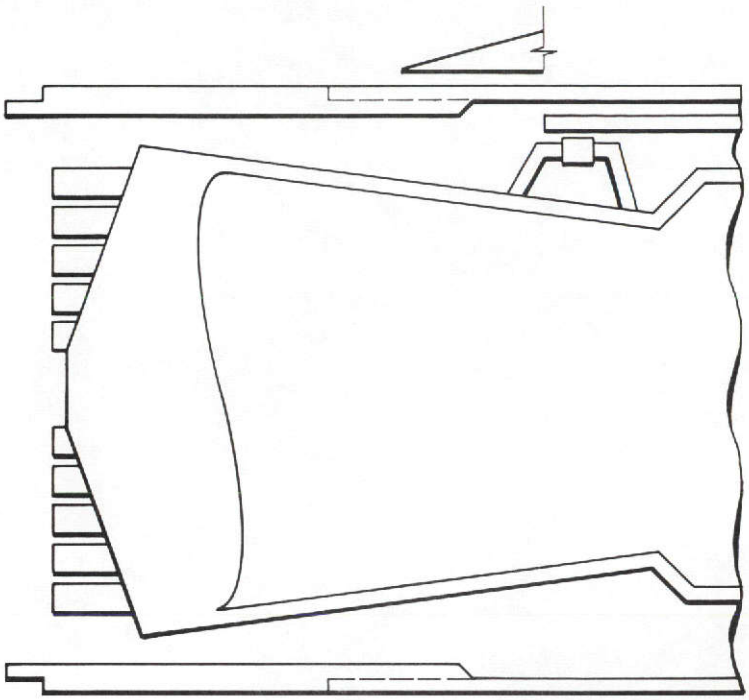

Figure 5(a).

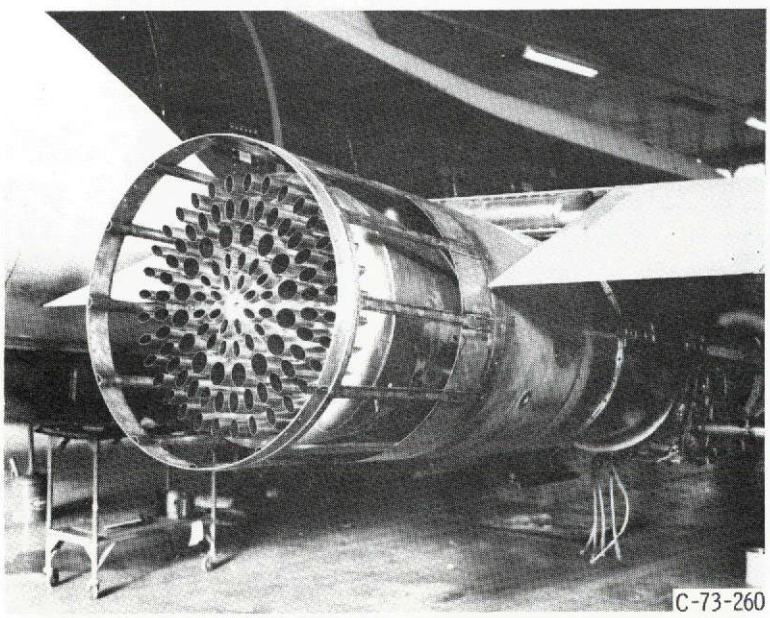


(a) WITHOUT SHROUD

Figure 5. - Suppression nozzle.

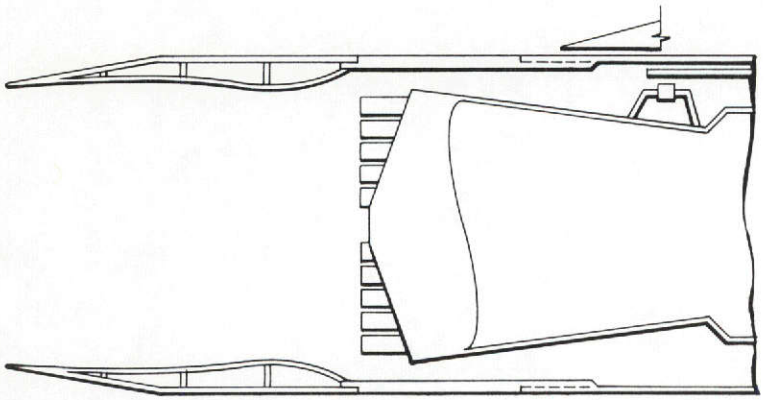

Figure 5(b).


(b) WITH ACOUSTIC SHROUD

Figure 5. - Concluded.

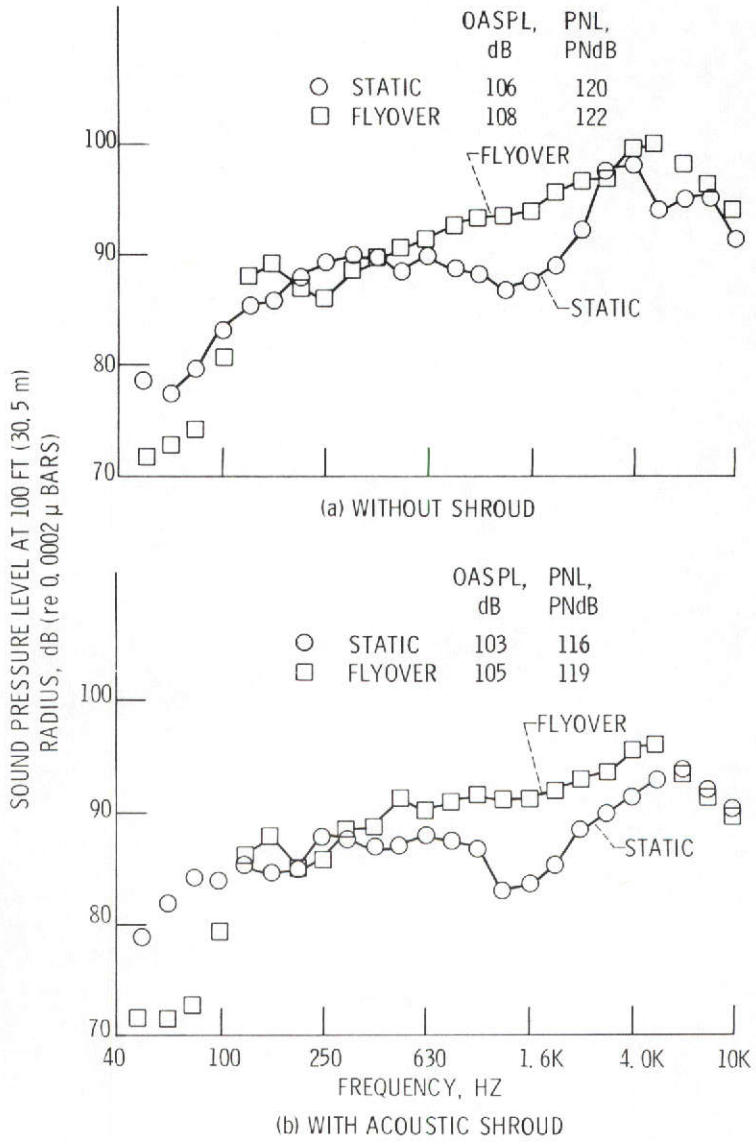


Figure 6. - Comparison of flyover and static spectra at the same relative jet velocity, $V_r$ = 1760 ft/sec (536 m/sec); $\theta = 70^0$; 1/3-octave bands. Free-field; standard day.

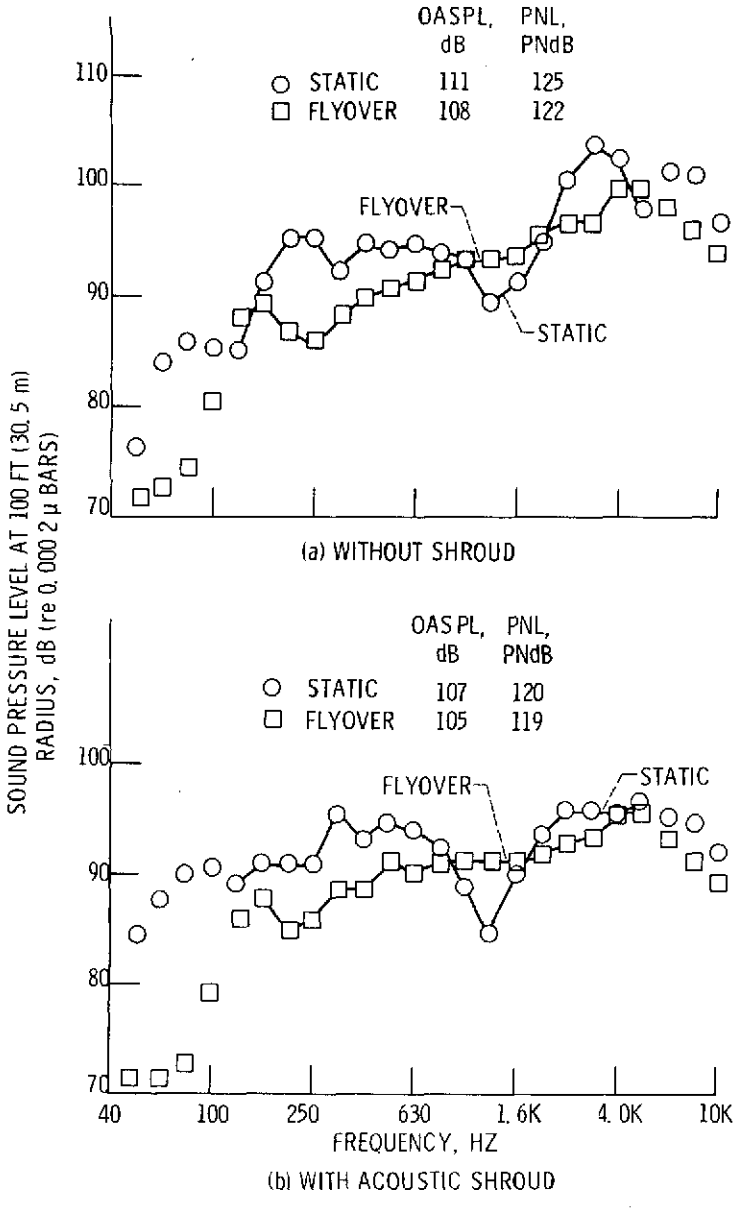


Figure 7. - Comparison of flyover and static spectra at the same jet velocity, $V_j$ = 2200 ft/sec (670 m/sec); $\theta = 70^0$; 1/3-octave bands; free-field; standard day.

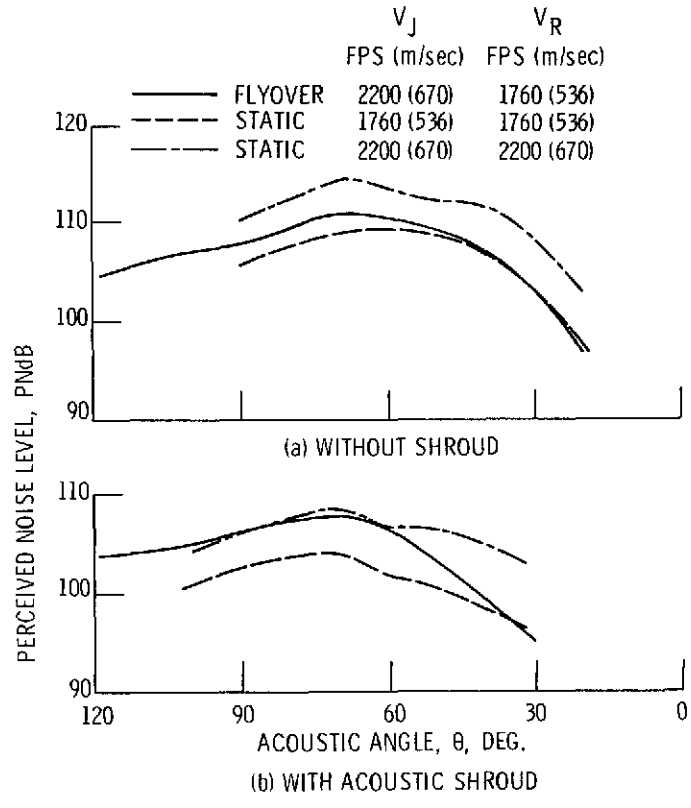


Figure 8. - Flyover and static directivity of 104-tube suppressor, 300 ft (91 m) altitude/sideline. Free-field; standard day.

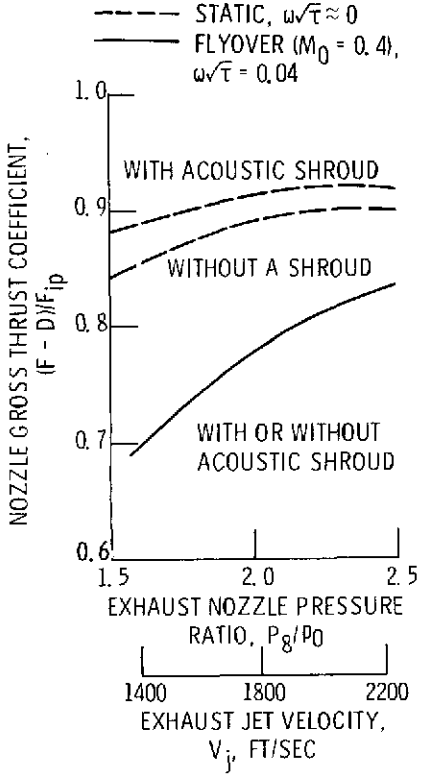


Figure 9. - Nozzle gross thrust coefficient of 104-tube suppressor.

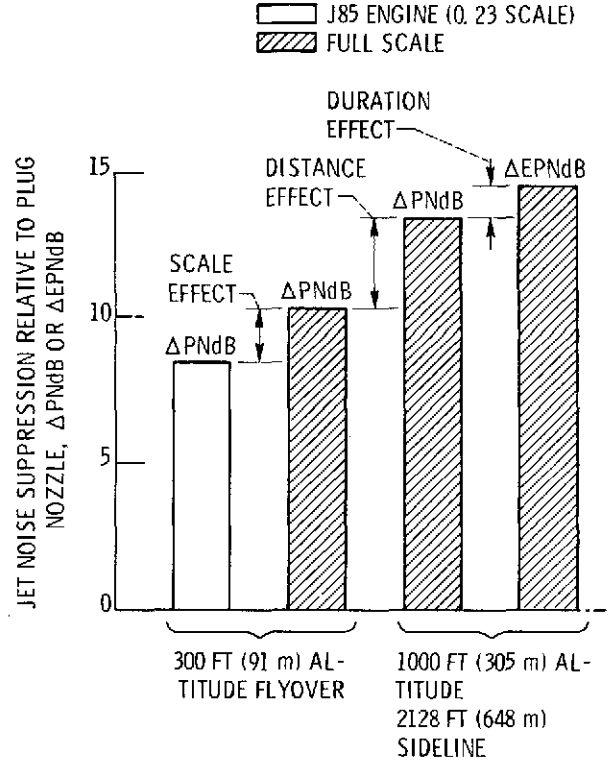


Figure 10. - Effect of scale, distance, and duration on suppression of 104-tube suppressor with acoustic shroud.

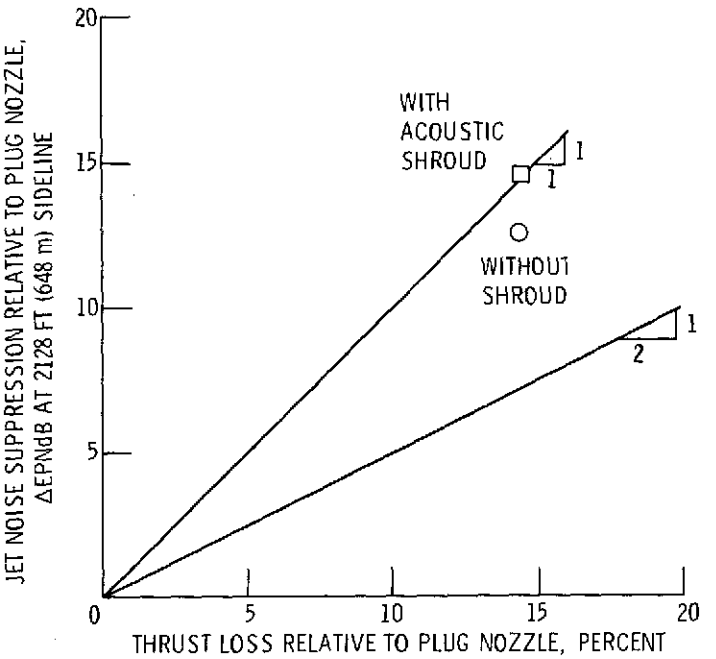


Figure 11. - Effectiveness of 104-tube suppressor scaled to full size engine, 2128 ft (648 m) sideline, 1000 ft (305 m) altitude, 0.4 Mach number.

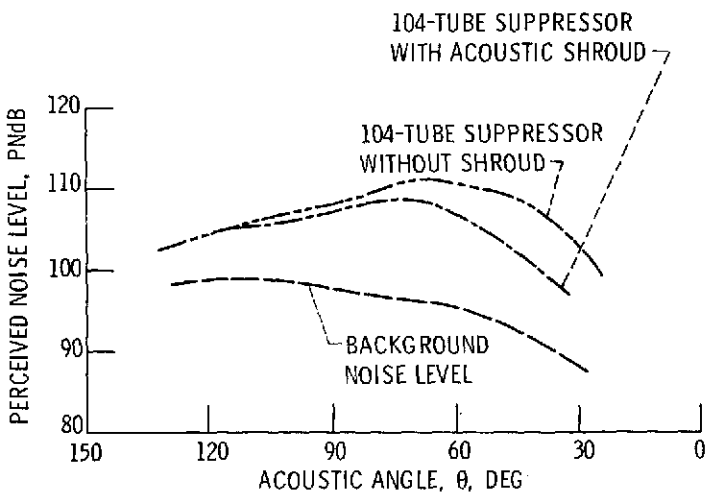


Figure 12. - Background noise level during flyover. 300 ft (91 m) altitude, 0.4 Mach number; free-field; standard day.

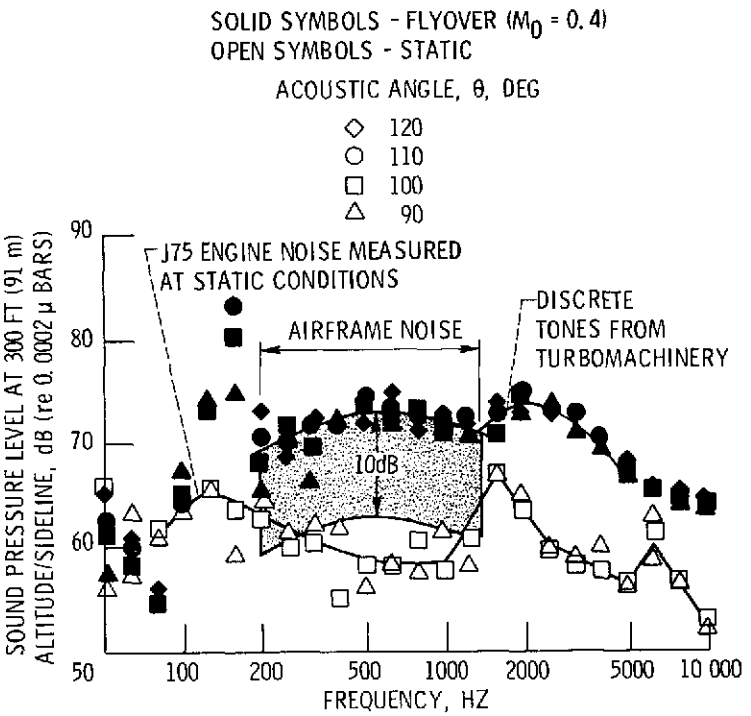


Figure 13. - Flyover and static spectra of background noise level. Free-field; standard day.

E-2023

| | PEAK FREQ., HZ | OASPL, dB |
|---|---|---|
| FLIGHT DATA, F-106 | 570 | 83[1] |
| CALC. FROM EQ., REF. 4 | 530 | 105 |

[1]ADJUSTED TO FREE-FIELD

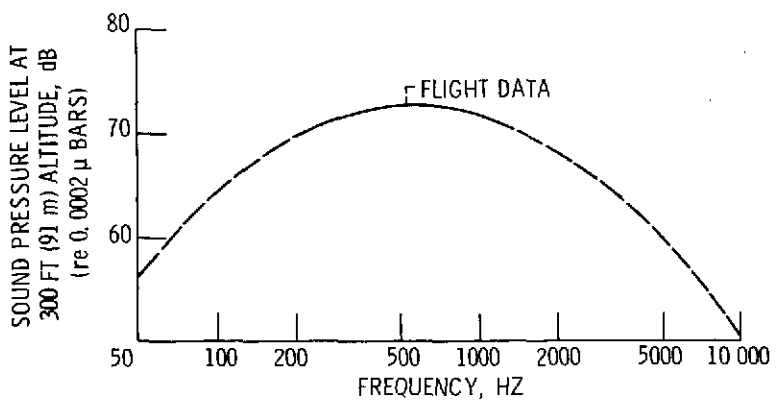


Figure 14. - Comparison of measured and predicted airframe noise; 0.4 Mach number; standard day.

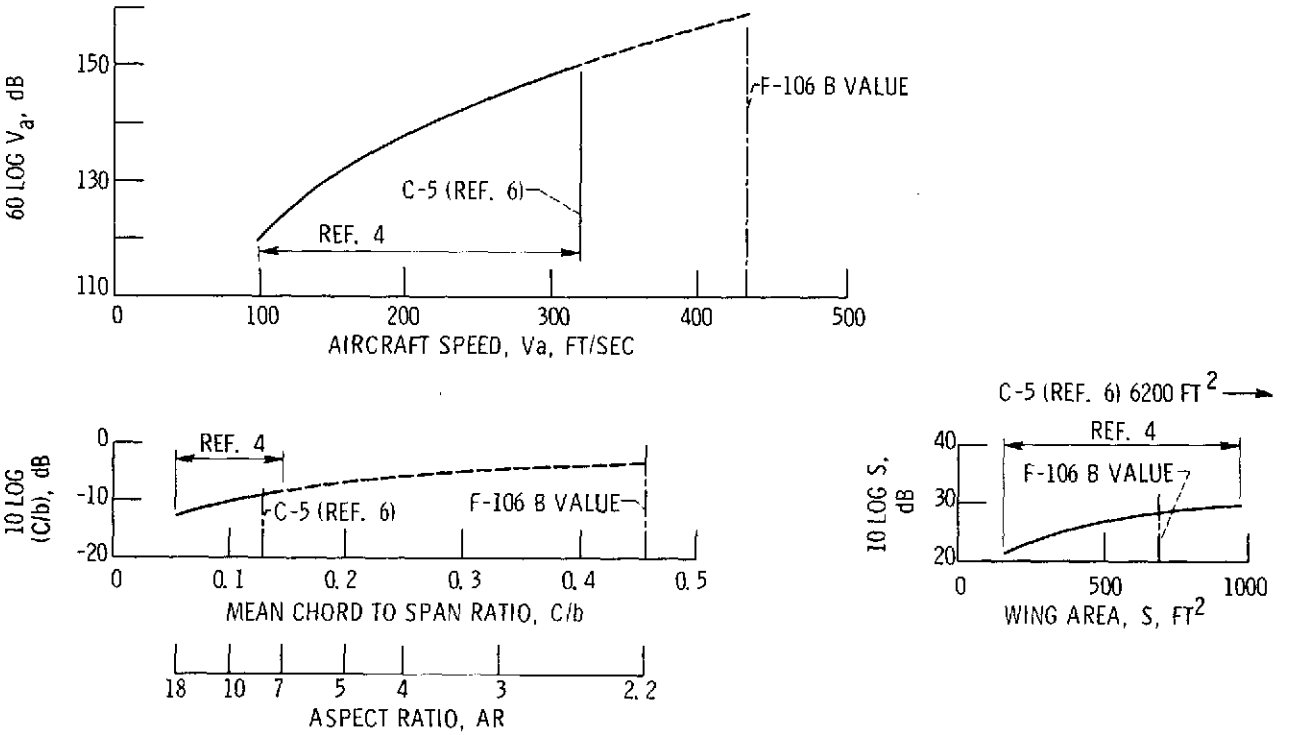


Figure 15. - The range over which aircraft parameters were investigated in reference 4 compared with values for the F-106 B test, and the C-5 galaxy of reference 6.